CrossMark

ORIGINAL PAPER

New class of chaotic systems with equilibrium points like a three-leaved clover

Saleh Mobayen [ORCID] · **Christos K. Volos** ·
Sezgin Kaçar · **Ünal Çavuşoğlu**

Abstract This paper presents a new class of chaotic systems with infinite number of equilibrium points like a three-leaved clover. They signify an exciting class of dynamical systems which represent many major characteristics of regular and chaotic motions. These chaotic systems belong to the general class of chaotic systems with hidden attractors. By using a systematic computer search, three chaotic systems with three-leaved-clover-shaped equilibria were found which are classified into dissipative systems. Dynamics of the chaotic system with the three-leaved-clover-equilibria has been investigated by using phase portraits, bifurcation diagram, Lyapunov exponents, Kaplan–Yorke dimension and Poincaré map. Moreover, an electronic circuit implementation of the theoretical system is designed to check its effectiveness. Random number generator design has been realized with newly developed chaotic systems. The obtained random bit sequences are used for image encryption. Security analysis of image encryption processes has been performed.

Keywords Chaotic system · Equilibrium point · Circuit design · Random number generator · Image encryption

1 Introduction

In the past years, a considerable amount of literature has been published on chaotic systems, for instance, Lorenz's system [1], Rössler's system [2], Sprott's system [3], Chen and Ueta's system [4], Chua's circuit [5], Linz and Sprott's system [6], Lü and Chen [7], Pehlivan and Uyaroglu [8], and so on. Since then, chaos theory has become a significant research issue in many chaos-based processes and information systems [9–15]. The complexity of chaotic systems has been applied in various engineering applications from image encryption [16–18], control and synchronization [19–25], weak signal detection [10] and forecasting water inrush in mines [26] to secure communication [27–29], cryptosystem design [30], audio encryption [31], permutation flow-shop scheduling problem [32], parallel distributed processing [33], and chaotic MIMO radar waveform design [34]. In the study of chaos, it is significant to form novel chaotic systems based on existing chaotic attractors. Chaotic systems have extremely complex nonlinear dynamics [35,36]. The fundamental specification of these systems is high sen-

S. Mobayen (✉)
Department of Electrical Engineering, Faculty of
Engineering, University of Zanjan, Zanjan, Iran
e-mail: mobayen@znu.ac.ir
http://www.znu.ac.ir/members/mobayen_saleh

C. K. Volos
Department of Physics, Aristotle University of
Thessaloniki, 54124 Thessaloniki, Greece

S. Kaçar
Department of Electrical and Electronics Engineering,
Sakarya University, Sakarya, Turkey

Ü. Çavuşoğlu
Department of Computer Engineering, Sakarya University,
Sakarya, Turkey

sitivity to parametric uncertainties and initial states. A smooth autonomous chaotic system can exhibit attractors with different numbers of wings disregarding the number of equilibria [37,38]. In fact, creation of complex multi-wing or multi-scroll chaotic attractors from three-dimensional autonomous systems has achieved rapid development [39,40]. In terms of difficulty, formation of a three-dimensional autonomous system with a complex attractor is an important and stimulating task in theory and practical purposes [41]. Due to the above-mentioned properties of chaotic systems, chaos theory is employed in various scientific researches.

It is now well recognized from a variety of investigations that equilibrium points play important roles in theoretical design and dynamical analysis of chaotic systems [42,43]. An equilibrium point of a dynamical system is the real solution of the differential equation $\dot{x} = f(x) = 0$. The conventional chaotic systems have a countable number of equilibrium points. In recent years, a few strange chaotic systems with uncountable equilibrium points have been introduced [44]. There are three families of chaotic systems with infinite number of equilibria: systems with line equilibria [45–49], systems with open-curve equilibria [50,51], and systems with closed-curve equilibria [52–54]. The considerable properties of systems with infinite number of equilibria are rare and challenging to find. It is recognized that such systems with infinite number of equilibrium points exhibit hidden attractors, which have been studied as an exciting research subject in the recent years [55–58]. Nevertheless, there is still a necessity to discover new chaotic systems with different closed-curve equilibria [59,60].

In this paper, a new chaotic system with infinite number of equilibria like a three-leaved clover is proposed. Using a systematic computer search, three dissipative chaotic systems with three-leaved-clover-shaped equilibria are found. To help understand the chaos generation of this system, some dynamical specifications containing phase portraits, bifurcation diagram, Lyapunov exponents, Kaplan–Yorke dimension and Poincaré map are discussed exhaustively. Furthermore, to investigate the applicability of the new chaotic system, an electronic circuit implementation and an RNG design are realized and the achieved random bit sequences are employed for image encryption. Finally, security analysis of image encryption processes has been executed.

This paper is organized as follows: In Sect. 2, the mathematical model of the new chaotic system is pro-

posed. In Sect. 3, some discussion for the chaotic system containing dynamical specifications such as bifurcation diagrams, Lyapunov exponents, Kaplan–Yorke dimension, and Poincaré map is presented. An electronic circuit realization of the new chaotic system is performed in Sect. 4, while its engineering applications comprising the RNG design and image encryption are reported in Sect. 5. Finally, the last section presents conclusions of overall study.

2 Mathematical model of the chaotic system

In the search for chaotic flows with infinite number of equilibrium points, we consider the model of a novel three-dimensional chaotic system with equilibrium points like a three-leaved clover as

$$
\begin{aligned}
\dot{x} &= a_1 z \\
\dot{y} &= -z f_1(x, y, z) \\
\dot{z} &= f_2(x, y),
\end{aligned}
\tag{1}
$$

where x, y, and z signify the state variables and $f_1(x, y, z)$ and $f_2(x, y)$ specify the nonlinear functions as:

$$
\begin{aligned}
f_1(x, y, z) &= a_2 x + a_3 y + a_4 z + a_5 x^2 + a_6 y^2 \\
&\quad + a_7 z^2 + a_8 xy + a_9 xz + a_{10} yz + a_{11},
\end{aligned}
\tag{2}
$$

$$
f_2(x, y) = x^4 + 2x^2 y^2 + y^4 - x^3 + 3xy^2,
\tag{3}
$$

where $[a_1, a_2, \ldots, a_{11}]$ are the constant parameters.

The equilibrium of the general model (1) can be found as:

$$
\begin{aligned}
z &= 0, \\
z \, f_1(x, y, z) &= 0, \\
f_2(x, y) &= 0,
\end{aligned}
\tag{4}
$$

where it is concluded that in the plane $z = 0$, the equilibrium points of the general model (1) lay on the surface $f_2(x, y) = 0$. Then, it is confirmed that the system (1) has infinite number of equilibrium points $E(x^*, y^*, 0)$ located on

$$
x^{*4} + 2x^{*2} y^{*2} + y^{*4} - x^{*3} + 3x^* y^{*2} = 0.
\tag{5}
$$

Interestingly, Eq. (5) defines a three-leaved-clover-shaped curve of equilibrium points, as shown in Fig. 1.

An exhaustive computer search is performed considering millions of combinations of the parameters $a_1, \ldots, a_{11}$ and initial conditions, seeking for the

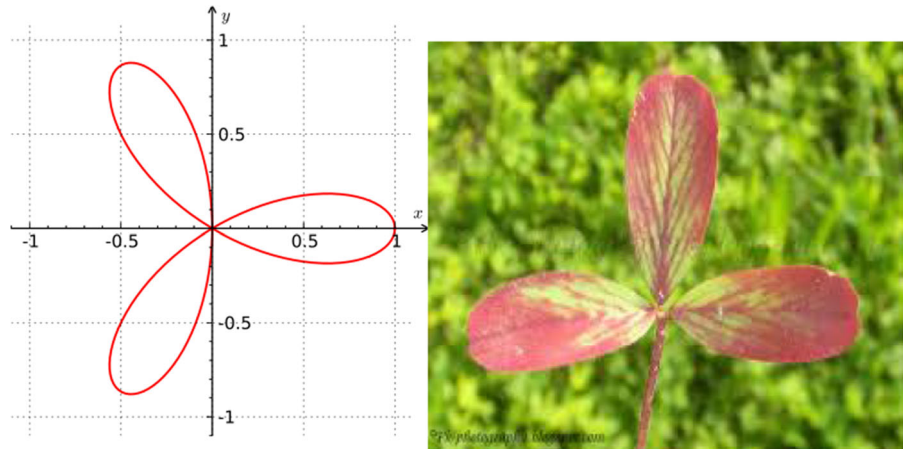**Fig. 1** Presentation of the three-leaved-clover–shaped equilibrium

Table 1 Three chaotic flows with equilibrium points like a three-leaved clover

Case	Dynamics	Parameters	Lyapunov exponents	D_{KY}	(x_0, y_0, z_0)
CL1	$\dot{x} = az$ $\dot{y} = -z(by + z^2 + yz)$ $\dot{z} = x^4 + cx^2y^2 + y^4 - x^3 + dxy^2$	$a = 0.29$	0.0130 ± 0.0051	2.1727	$(-0.54, -0.69, 0.37)$
		$b = 1.4$	0		
		$c = 2$	-0.0753		
		$d = 3$			
CL2	$\dot{x} = az$ $\dot{y} = -z(by + x^2 + cyz)$ $\dot{z} = x^4 + dx^2y^2 + y^4 - x^3 + exy^2$	$a = 0.3$	0.0139 ± 0.0045	2.1565	$(-0.29, 0.37, 0.2)$
		$b = 1.8$	0		
		$c = d = 2$	-0.0887		
		$e = 3$			
CL3	$\dot{x} = az$ $\dot{y} = -z(bx + cy + dyz)$ $\dot{z} = x^4 + ex^2y^2 + y^4 - x^3 + fxy^2$	$a = 0.15$	0.0052 ± 0.0025	2.1217	$(0.19, 0.29, -0.34)$
		$b = 0.2$	0		
		$c = d = e = 2$	-0.0423		
		$f = 3$			

chaotic behavior with the largest Lyapunov exponent greater than 0.001. Cases CL1–CL3 in Table 1 are three chaotic systems obtained in this way. In addition to the cases CL1–CL3, dozens of chaotic systems with more complicated structures and inessential terms were found. Figure 2 demonstrates the strange chaotic attractors of the cases CL1–CL3 with infinite number of equilibria like a three-leaved clover.

Since the sum of the Lyapunov exponents of chaotic systems CL1–CL3 is negative, one can conclude that the new chaotic systems CL1–CL3 are dissipative. The

equilibrium points, Lyapunov exponents, and Kaplan–Yorke dimensions are reported in Table 1 along with the initial states which are close to the chaotic attractors. As is common for strange chaotic attractors of three-dimensional autonomous systems, the dimensions of the attractors for the cases CL1–CL3 are only slightly greater than 2. Among dissipative cases CL1–CL3, the largest Kaplan–Yorke dimension is 2.1727 for CL1, although no effort is done to tune the parameters for high complexity.
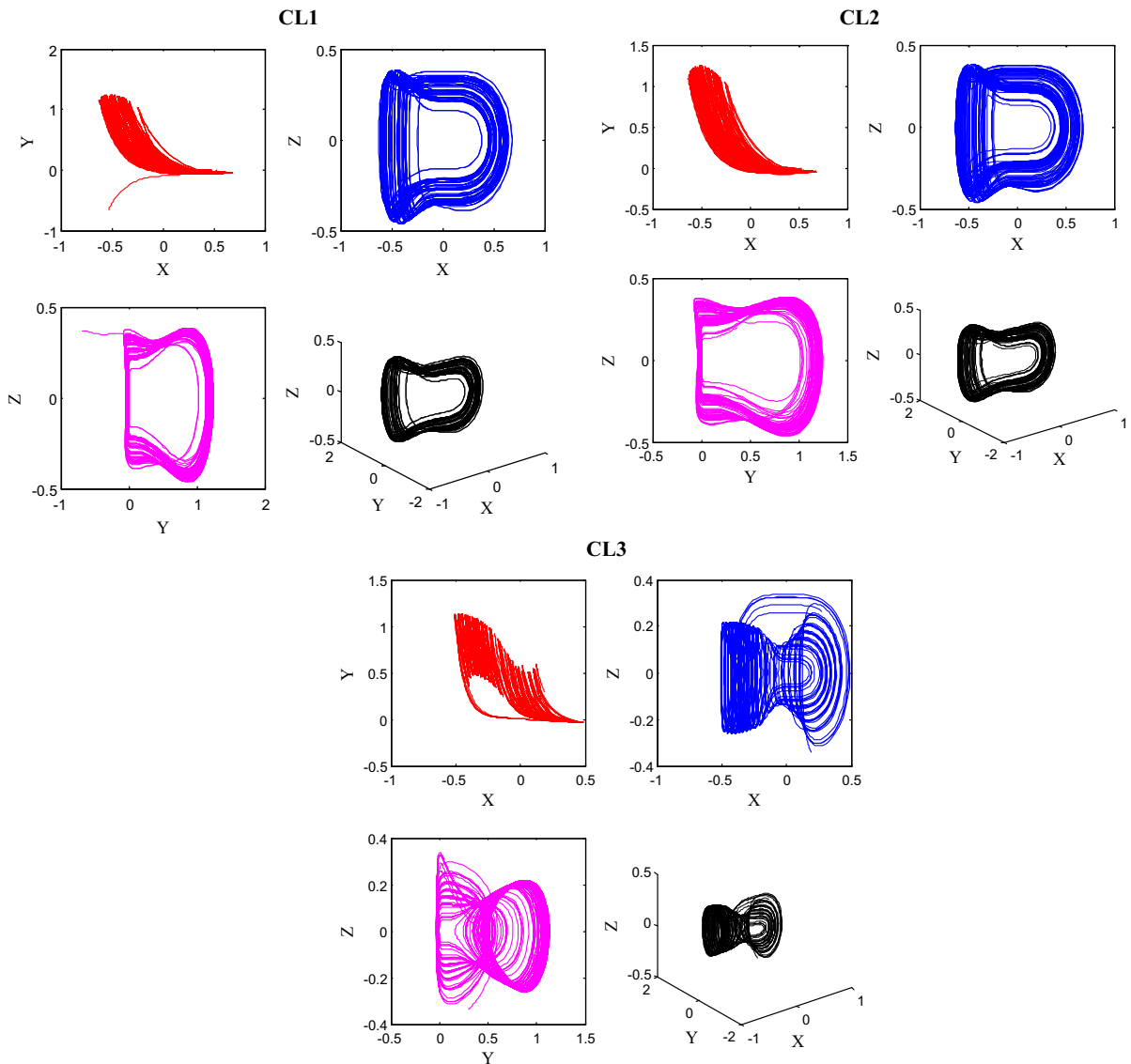
Fig. 2 Strange chaotic attractors of cases CL1–CL3

3 Discussions

In this section, we study further as a simple example the system CL1 due to the fact that it has the biggest value of Kaplan–Yorke dimension (D_{KY}). By investigating the effect of CL1's parameters (b, c and d) of nonlinear terms on system's behavior, our simulations indicated that CL1 system displays striking dynamics. Firstly, the value of the parameter b is varying in the range from 1.3 to 1.7 in order to show the dynamics of system CL1 by obtaining the bifurcation diagram

of the variable z when the trajectories cut the plane $x = 0$ with $dx/dt < 0$, as the control parameter b is decreased. For this reason, the proposed system CL1 is integrated numerically using the classical fourth-order Runge–Kutta integration algorithm. For each set of parameters used in this work, the time step is always $\Delta t = 0.002$ and the calculations are performed using variables and parameters in extended precision mode. For each parameter settings, the system is integrated for a sufficiently long time and the transient is discarded.
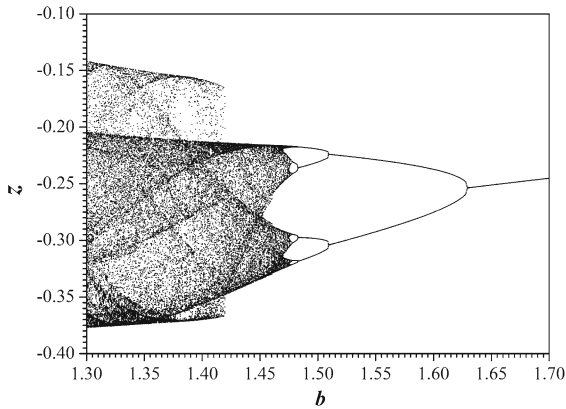
Fig. 3 Bifurcation diagram of z versus b of the system CL1, for $a = 0.29$, $c = 2$ and $d = 3$

Fig. 4 Lyapunov exponents of the system CL by varying the parameter b, for $a = 0.29$, $c = 2$, and $d = 3$

The bifurcation diagram and the three Lyapunov exponents of the system CL1 are presented in Figs. 3 and 4, respectively. Here, Lyapunov exponents are calculated with the Wolf's algorithm [61]. As can be seen from Figs. 3 and 4, there is the presence of a classical period-doubling route to chaos when decreasing the value of the parameter b. For $b \geq 1.476$, system CL1 generates periodical oscillations. For instance, period-1, period-2, period-4, and period-8 oscillations of system CL1 are illustrated in Fig. 5, respectively. For $b < 1.476$, system CL1 displays more complex behaviors, for example chaos (see the strange attractors of system CL1 in Fig. 2). The Poincaré map of system CL1 in y–z plane, when $x = 0$ with $\mathrm{d}x/\mathrm{d}t < 0$ (see Fig. 6), also indicates the properties of chaos. Finally, it is noted that the system is unbounded for $b < 1.216$.

Similarly, we have changed the value of the parameter c and d to discover the dynamics of system CL1. The bifurcation diagrams of system CL1 for $c \in [1.7, 3.1]$ and $d \in [2.5, 3.2]$ are reported in Fig. 7. As shown in Fig. 7, the presence of a classical period-doubling route to chaos is observed when decreasing the value of the parameter c and increasing the value of the parameter d. Furthermore, the corresponding spectrums of the three Lyapunov exponents by varying the parameter c and the parameter d are shown in Fig. 8. It can be seen that the bifurcation diagrams well coincide with the spectrum of the Lyapunov exponents.

4 Circuit realization

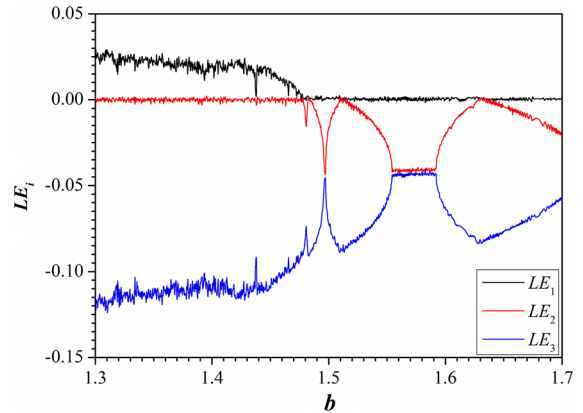The classical approach for the verification of the feasibility of theoretical chaotic models is the physical realization through electronic circuits [62–66]. Furthermore, the circuital realization of chaotic systems has been applied in numerous engineering applications, for example in secure communications [67,68], liquid mixing [69], robotics [70], image encryption process [71], audio encryption scheme [31], target detection [72], or random signal generation [73,74]. For this reason, analog and digital approaches have been applied to realize chaotic oscillators by using different kinds of electronic devices such as common off-the-shelf electronic components [75,76], integrated circuit technology [77,78], microcontroller [79], or field-programmable gate array (FPGA) [80–82].

Therefore, in this section, we will confirm the feasibility of one of the proposed systems CL1–CL3 by discussing its circuital realization by using the general operational amplifier-based approach. In more details, the system which has been chosen in this work is the system CL1. The three state variables (x, y, z) of the system CL1 have been rescaled as $X = 10x$, $Y = 5y$, and $Z = 10z$, in order to avoid the limitations of the components of electronic circuit. Therefore, the system CL1 is transformed into the following equivalent system:

$$\dot{X} = 0.29Z$$
$$\dot{Y} = -Z\left(\frac{1.4}{10}Y + \frac{Z^2}{200} + \frac{YZ}{100}\right)$$
$$\dot{Z} = \frac{X^4}{1000} + \frac{2X^2Y^2}{250} + \frac{Y^4}{62.5} - \frac{X^3}{100} + \frac{3XY^2}{25} \quad (6)$$

Figure 9 shows the schematic of the circuit for realizing the system (6). As shown in this figure, the circuit includes nine resistors, three capacitors, four oper-
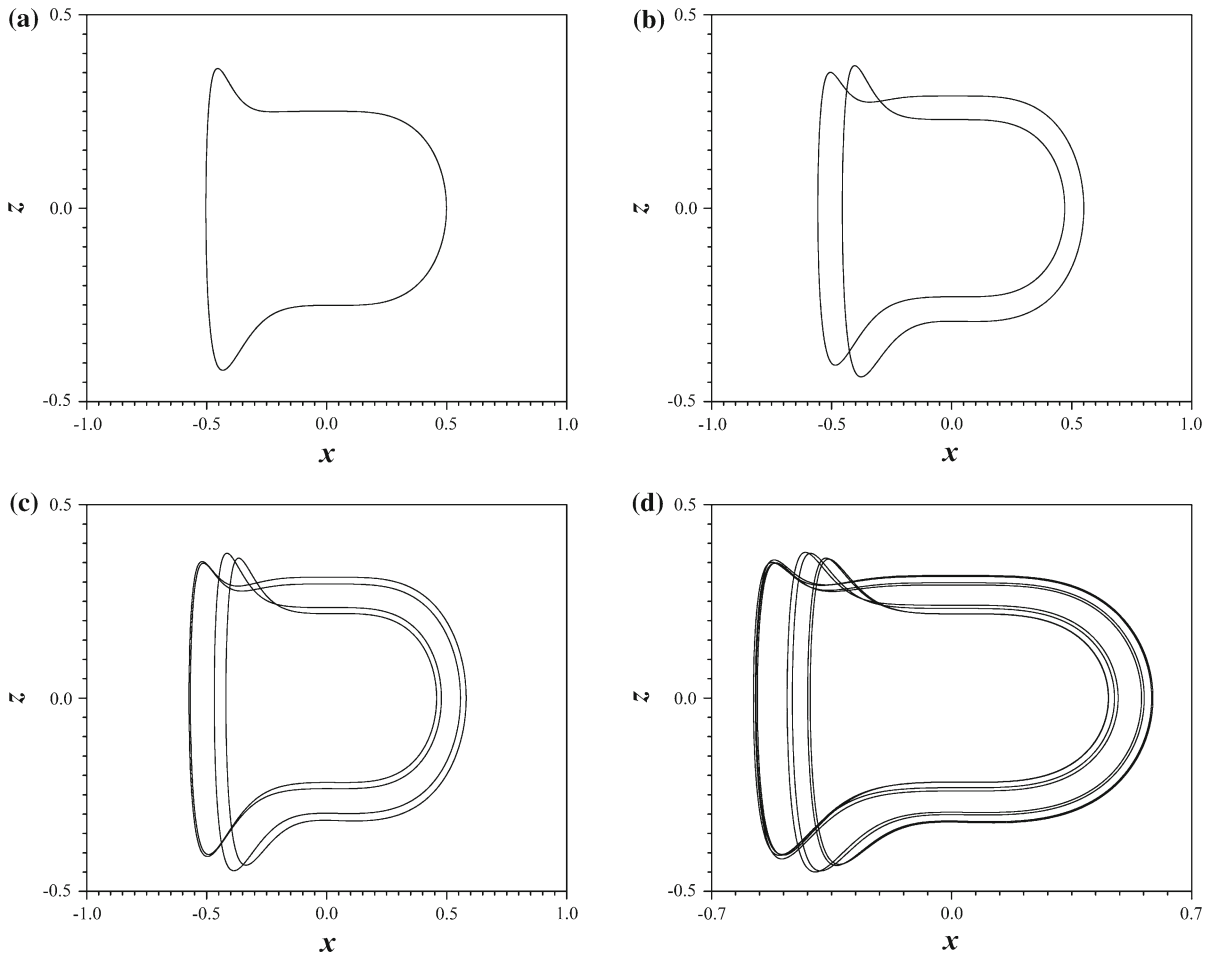
(a)

(b)

(c)

(d)

Fig. 5 Four views of periodic behaviors of the system CL1: **a** period-1 oscillation ($b = 1.65$), **b** period-2 oscillation ($b = 1.55$), **c** period-4 oscillation ($b = 1.49$), **d** period-8 oscillation ($b = 1.48$), for $a = 0.29$, $c = 2$ and $d = 3$
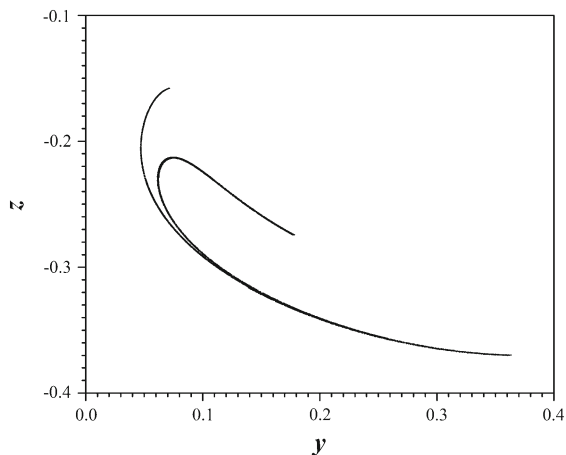
Fig. 6 Poincaré map of system CL1 in the y–z plane, for $a = 0.29$, $b = 1.4$, $c = 2$ and $d = 3$

ational amplifiers (TL081), and eleven analog multipliers (AD633). In this point, we should mention that the most common nonlinearities in chaotic oscillators are polynomials or the products of two state variables, as it happened in system CL1. For this reason, nonlinear circuits designed from a mathematical chaotic system usually require analog multipliers, such as AD633. In fact, despite the accuracy of analog devices, the non-ideal effects are always present. The nonidealities of the analog multipliers may lead to further nonlinear terms, which will be considered as parasitic effects [83]. However, in this work, the parasitic effects of the analog multipliers have been neglected because according to our study, they do not affect significantly circuit's behavior in regard to the expected behavior from the numerical simulation.
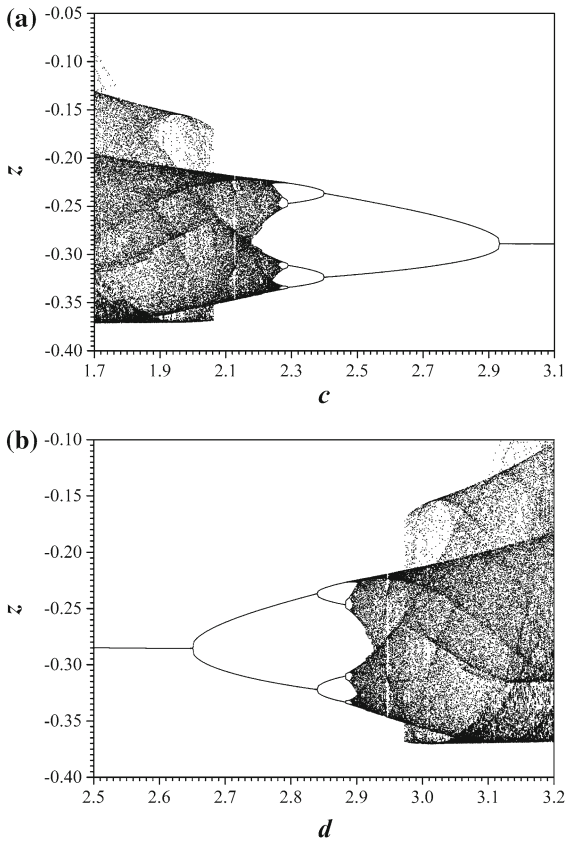
Fig. 7 Bifurcation diagrams of **a** z versus c and **b** z versus d, of the system CL1
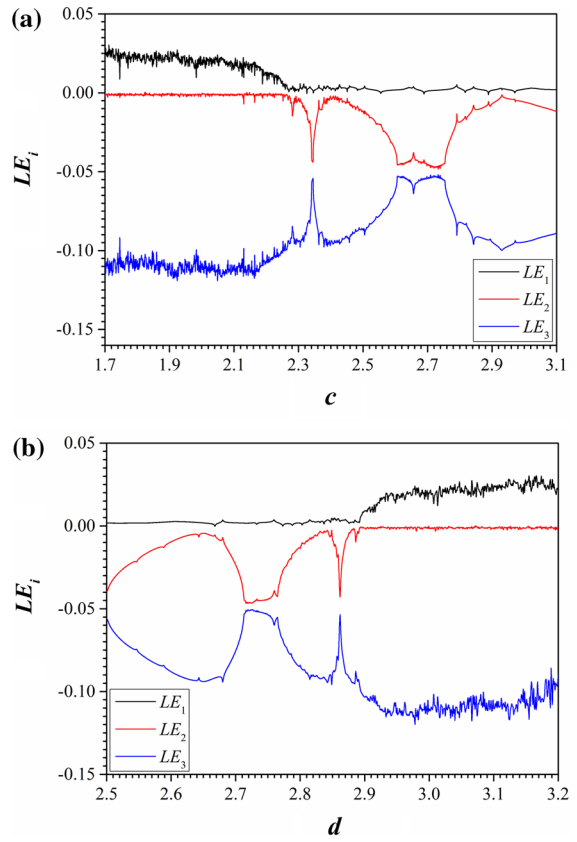

Fig. 8 Lyapunov exponents of the system CL1, by varying **a** the parameter c and **b** the parameter d

By applying Kirchhoff's circuit laws into the designed circuit, we get the following circuital equation:

$$\dot{X} = \frac{1}{RC}\left(\frac{R}{R_1}Z\right)$$

$$\dot{Y} = \frac{1}{RC}\left(-\frac{R}{R_2 10V}YZ - \frac{R}{R_3 100V}Z^3\right.$$
$$\left. - \frac{R}{R_4 100V^2}YZ^2\right)$$

$$\dot{Z} = \frac{1}{RC}\left(\frac{R}{R_5 1000V^3}X^4 + \frac{R}{R_6 1000V^3}X^2Y^2\right.$$
$$+ \frac{R}{R_7 1000V^3}Y^4 - \frac{R}{R_8 100V^2}X^3$$
$$\left. + \frac{R}{R_9 100V^2}XY^2\right) \quad (7)$$

In system (7), X, Y, and Z correspond to the voltages on the integrators (U2–U4), respectively, while the power supply is $\pm 15V_{DC}$. System (7) is normalized by using $\tau = t/RC$. It can thus be suggested that

system (7) is equivalent to system (6), with $\frac{R}{R_1} = 0.29$, $\frac{R}{R_2} = 1.4$, $\frac{R}{R_3} = \frac{1}{2}$, $\frac{R}{R_4} = 1$, $\frac{R}{R_5} = 1$, $\frac{R}{R_6} = 8$, $\frac{R}{R_7} = 16$, $\frac{R}{R_8} = 1$, and $\frac{R}{R_9} = 12$. So, the values of circuit components are: $R = 10$ kΩ, $R_1 = 66.666$ kΩ, $R_2 = 7.143$ kΩ, $R_3 = R_4 = R_5 = R_8 = 1$ kΩ, $R_6 = 12.5$ kΩ, $R_7 = 0.625$ kΩ, $R_9 = 0.833$ kΩ, and $C_1 = C_2 = C_3 = C = 1$ nF. The designed circuit has been implemented in Multisim, and PSpice results are reported in Fig. 10. It is easy to see the agreement between the circuit's simulation results (Fig. 10) and numerical results (Fig. 2).

5 Engineering application (RNG design and image encryption)

In this section, an RNG algorithm is designed using the developed chaotic systems, and the random numbers obtained from the RNG algorithm are applied to NIST-800-22 [84] randomness tests. Then, an image
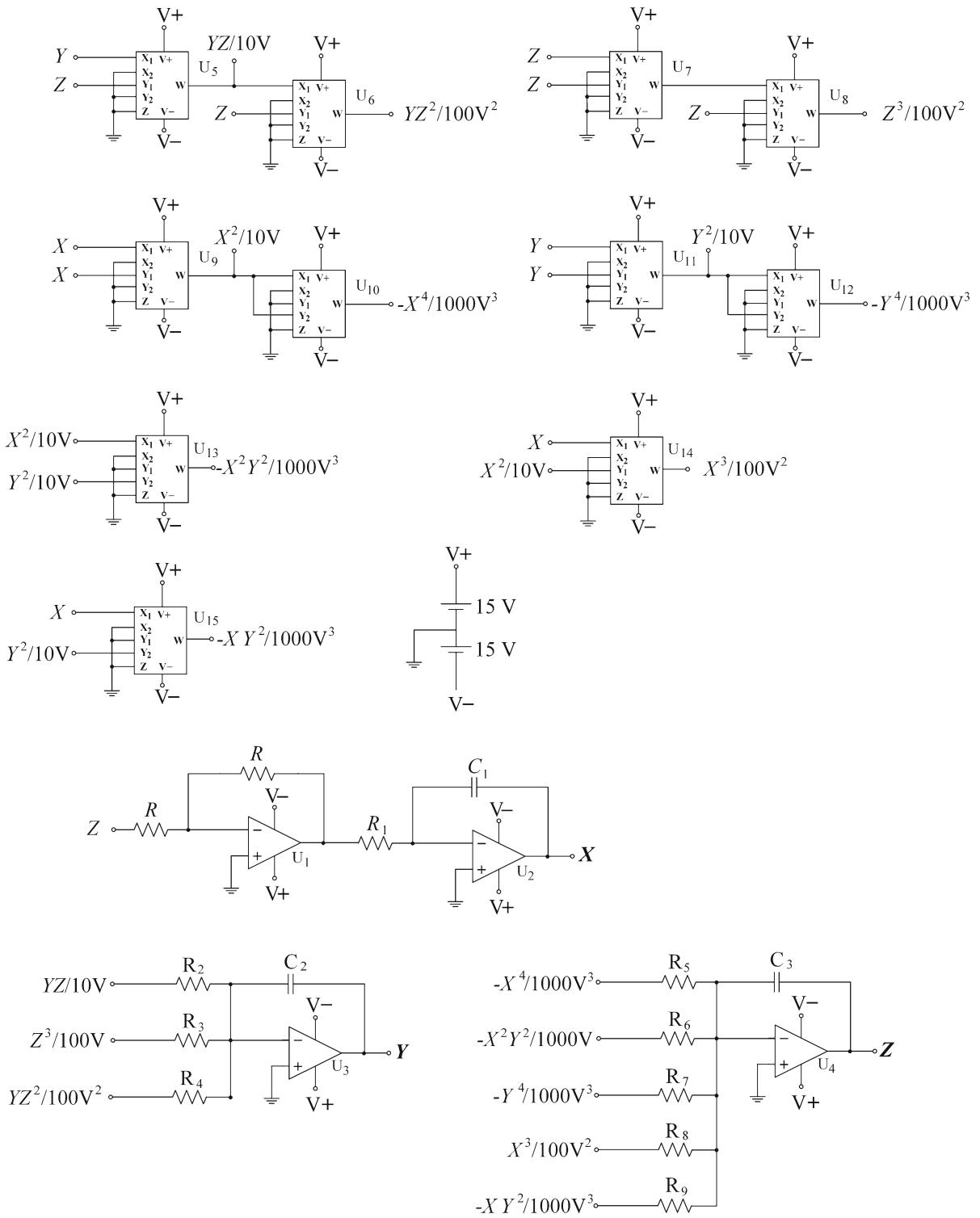
Fig. 9 Schematic of the circuit including nine resistors, three capacitors, four operational amplifiers, and eleven analog multipliers. The power supplies of all operational amplifiers and analog multipliers are $\pm 15 V_{DC}$

Fig. 10 PSpice chaotic attractors of the designed circuit in **a** X-Y plane, **b** X-Z plane, and **c** Y-Z plane
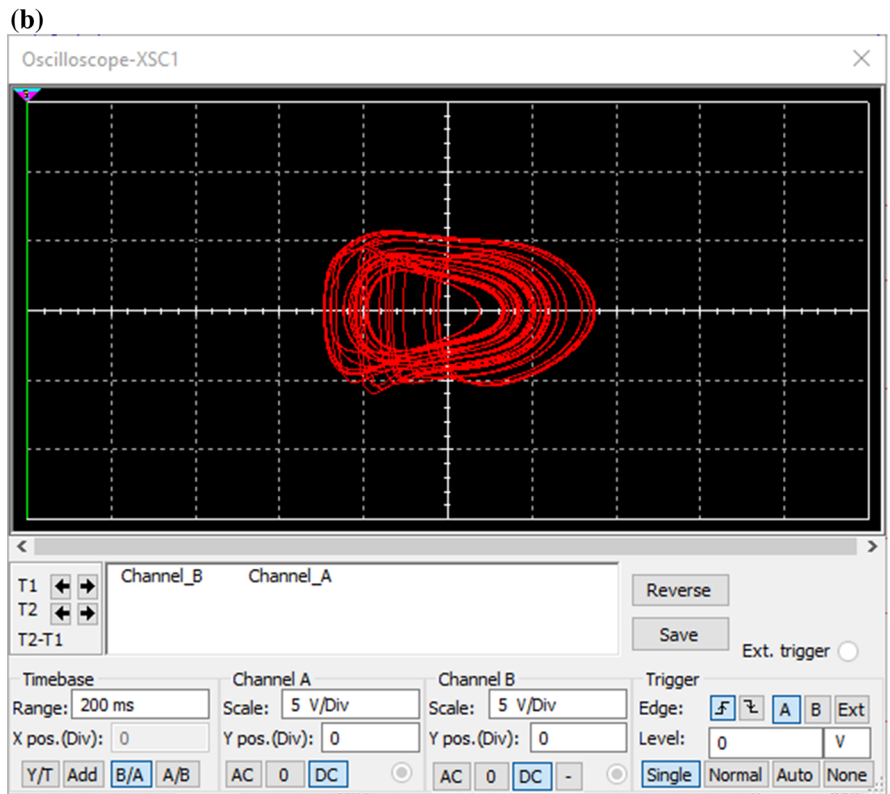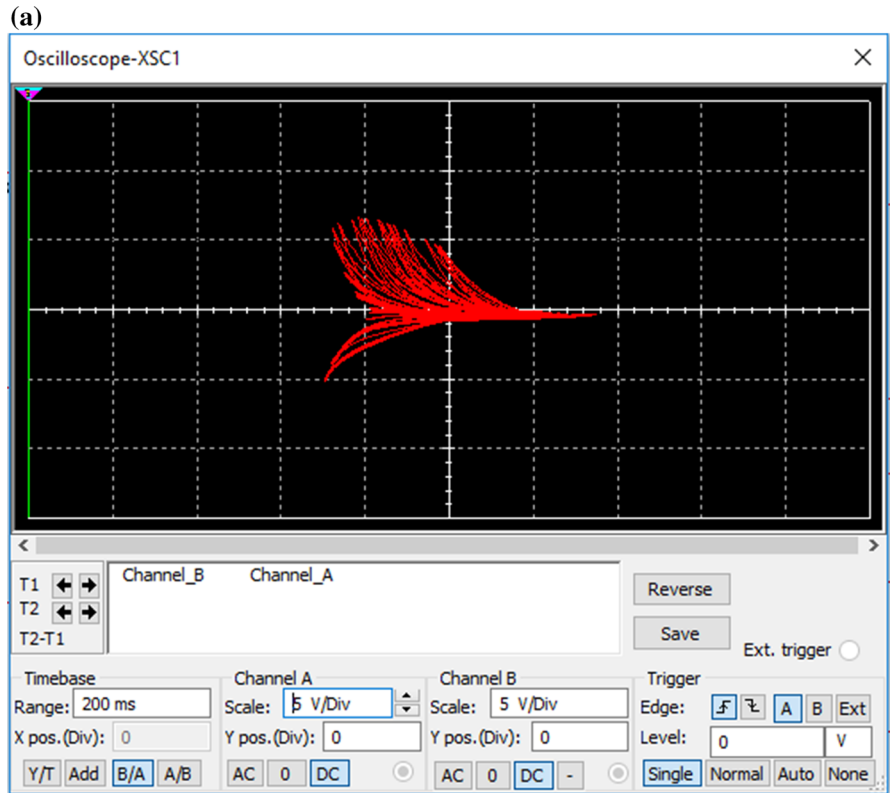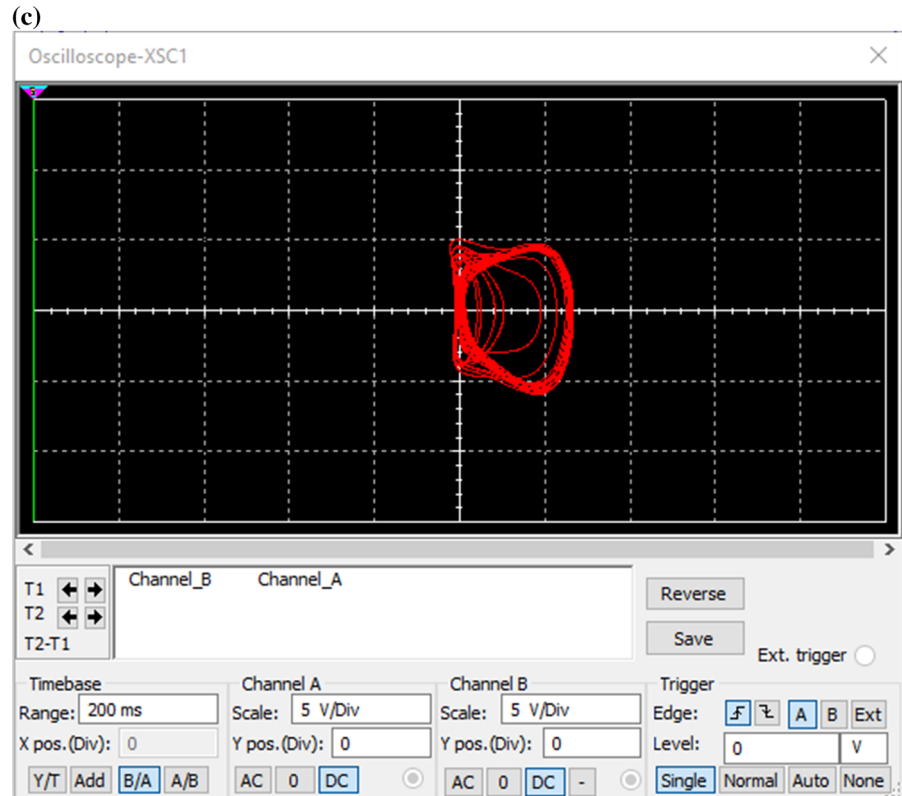
Fig. 10 continued

encryption algorithm with random bit sequences generated by the RNG algorithm is presented, and image encryption application is performed. Tests have been conducted to demonstrate the level of security of the image encryption process performed.

5.1 Design of RNG algorithm and NIST tests results

The random bit sequences to be used in the encryption process are very important for the security of the encryption. Chaotic systems are widely used in random number generation because of their rich dynamics. The design steps of the RNG algorithm are given below.

Step 1 Enter initial conditions and system parameters for each chaotic system
CL1 $\Rightarrow$ (-0.54, -0.69, 0.37), CL2 $\Rightarrow$ (-0.29, 0.37, 0.2), CL3 $\Rightarrow$ (0.19, 0.29, -0.34);
Step 2 Determination of sampling interval ($\Delta h = 0.5$);
Step 3 Analysis of chaotic system using RK4 algorithm;
Step 4 Using the sampling step interval, obtain the float value from the analyzed system;

Step 5 Convert 32-bit binary value to float value;
Step 6 Selecting the LSB-10 bit from the 32-bit number array and adding it to the random number sequence;
Step 7 For each phase until a 1 million-bit number sequence is obtained, repeat range step 3–6;
Step 8 Bitwise XOR operation of 1 M. bit sequences generated for each phase;
Step 9 Applying NIST tests to the obtained 1 M. random bit sequences;

The RNG algorithm described above is applied separately for each chaotic system, and NIST tests are applied by obtaining different random bit sequences from each chaotic system. NIST 800-22 tests are used to determine the randomness degrees of random bit sequences. In NIST 800-22 tests, random number sequences are subjected to 16 different tests. To have sufficient randomness of the sequence of bits, it must pass all tests. Table 2 shows the NIST 800-22 test results of the bit sequences obtained from the XOR operation of the random bit sequences obtained from the x, y, and z phases of three different chaotic systems. According

Table 2 NIST-800-22 test results of RNGs based on CL systems

Statistical Tests	CL1	CL2	CL3	Result
Frequency (monobit) test	0.520873	0.17446	0.68768	Succesful
Block-frequency test	0.76462	0.68078	0.22397	Succesful
Cumulative-sums test	0.63380	0.13966	0.63380	Succesful
Runs test	0.29444	0.56721	0.78088	Succesful
Longest-run test	0.71467	0.20211	0.87729	Succesful
Binary matrix rank test	0.94092	0.18814	0.32573	Succesful
Discrete Fourier transform test	0.66624	0.15227	0.71357	Succesful
Nonoverlapping templates test	0.783508	0.04629	0.08552	Succesful
Overlapping templates test	0.63813	0.34304	0.61684	Succesful
Maurer's universal statistical test	0.06464	0.12314	0.74249	Succesful
Approximate entropy test	0.67279	0.62586	0.59645	Succesful
Random-excursions test ($x = -4$)	0.98268	0.93372	0.67386	Succesful
Random-excursions variant test ($x = -9$)	0.70965	0.165966	0.75193	Succesful
Serial test-1	0.17813	0.633643	0.70001	Succesful
Serial test-2	0.30113	0.615642	0.66190	Succesfull
Linear complexity test	0.94499	0.01083	0.62377	Succesfull

to the test results, the bit sequences obtained from each chaotic system have passed all tests.

5.2 Image encryption algorithm and its applications

After the RNG algorithm design, the encryption process is performed using the obtained random bit sequences. The image pixel values to be encrypted in the encryption algorithm are converted into a binary bit sequence. With these values, bit sequences obtained from the developed RNG algorithm are subjected to XOR processing and encryption is performed. Three different encryption processes have been performed with random bit sequences obtained from each chaotic system. In Fig. 11a, 256 * 256 size pepper.jpg original image is shown. Fig. 11b–d shows the results of cryptography performed with random bit sequences from CL1, CL2, and CL3 chaotic systems, respectively. Figure 11e shows the decrypted image resulting from decryption. Comparing the results in Fig. 11, it can be said that the encryption and decryption processes have been successfully performed for all the processes.

5.3 Security analysis results

In this section, the security analysis results of the encryption processes are presented. Security analy-

sis reveals the quality of the encryption process. Histogram, correlation, entropy, and linear-differential attack (NPCR–UACI) analyses of cryptographic operations are performed in security analysis. Firstly, histogram distributions of cryptographic processes are examined. Figure 12 shows histogram distribution graphs of original, encrypted, and decrypted pictures. Following the encryption process, the number of pixel values in the image is almost equal, indicating that a good encryption is being performed. When the results in Fig. 12 are examined, it is seen that the encryption results of four different systems have a good histogram distribution.

Correlation coefficient analysis [85] examines the relationship between random variables in the encryption process. This relationship should not be linear. The correlation coefficient is calculated using the following equation. In the equation, x and y represent the values of two adjacent pixels in the image, and N is the number of selected pixel pairs.

$$E(x) = \frac{1}{N}\sum_{i=1}^{N} x_i,$$

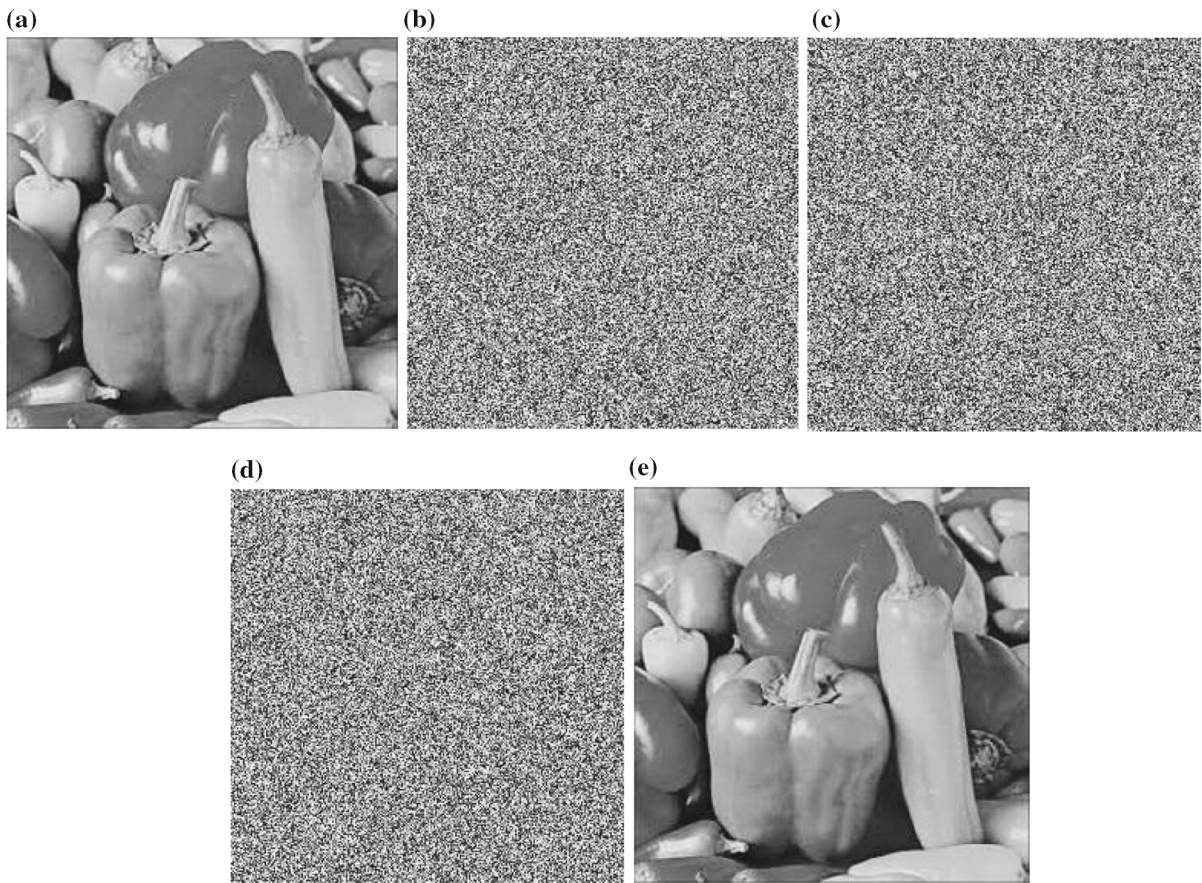$$D(x) = \frac{1}{N}\sum_{i=1}^{N} (x_i - E(x))^2,$$

Fig. 11 **a** Original image **b** CL1 encrypted image **c** CL2 encrypted image **d** CL3 encrypted image **e** decrypted image

$$\text{cov}(x, y) = \frac{1}{N} \left(\sum_{i=1}^{N} (x_i - E(x))(y_i - E(y)) \right),$$

$$r_{xy} = \frac{\text{cov}(x, y)}{\sqrt{D(x)D(y)}}. \tag{8}$$

The correlation graphs of the original and decrypted image are shown in Fig. 13a and f, respectively. These two graphs show that they are the same. Figure 13 shows the correlation distribution graphs of the encryption processes. Table 3 shows the correlation coefficient values of the encryption processes. When the graphs and the correlation coefficients are evaluated together, it is seen that the encryption processes have a good correlation distribution.

The complexity of the encrypted data is another criterion that gives information about the quality of the encryption. In information entropy analysis, the complexity of the encrypted data is determined. The formula used in information entropy analysis is

given below. The optimal information entropy value is accepted as 8 [86]. The closer the information is to the entropy value of 8, the better the quality of the encryption. In Table 3, information entropy values of all encryption processes are given. It seems that all of these values are very close to 8.

$$\text{Shan} En(x) = - \sum_{i=1}^{N} (p_i(x))^2 (\log_2 p_i(x))^2. \tag{9}$$

Number of pixels change rate (NPCR) and unified average changing intensity (UACI) [87] are cryptanalysis methods that are used to detect the resilience of the encryption process to differential attack attacks. The relation between the original and encrypted image is determined by the NPCR method. The equations used for NPCR calculation are given below. The NPCR optimal value is determined to be $\text{NPCR}_{\text{opt}} = 99.61\%$ [88].
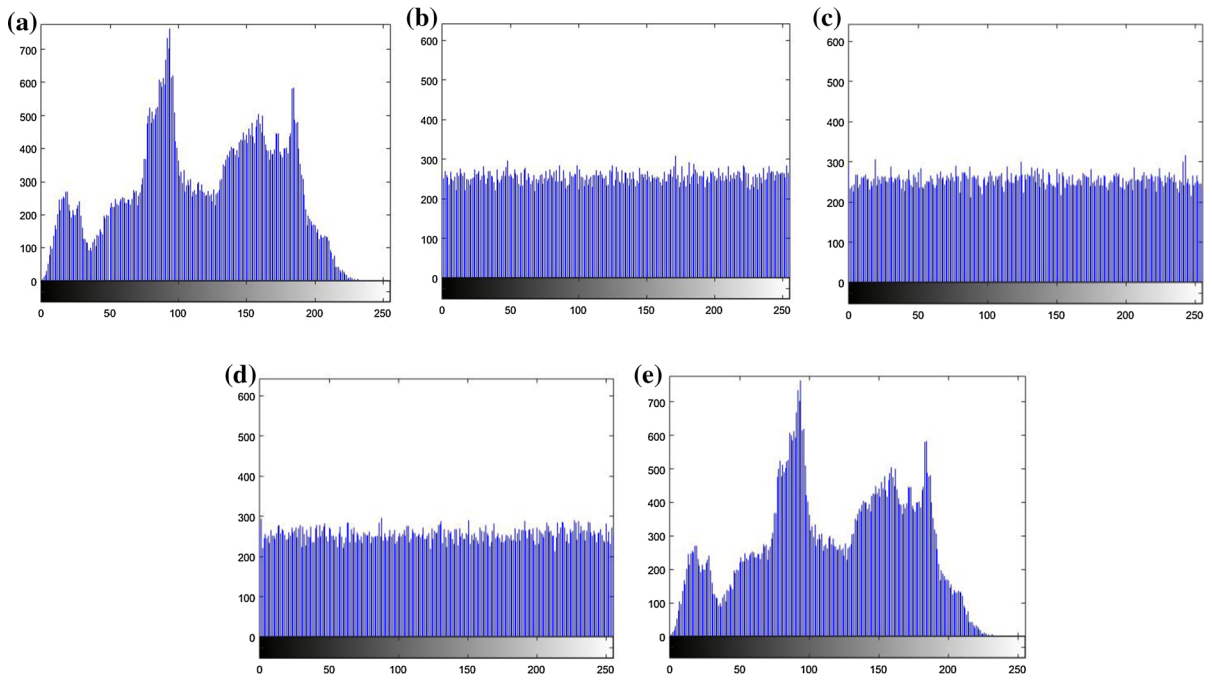
Fig. 12 The results of histogram analysis, **a** original image, **b** CL1 encrypted image, **c** CL2 encrypted image, **d** CL3 encrypted image, **e** decrypted image
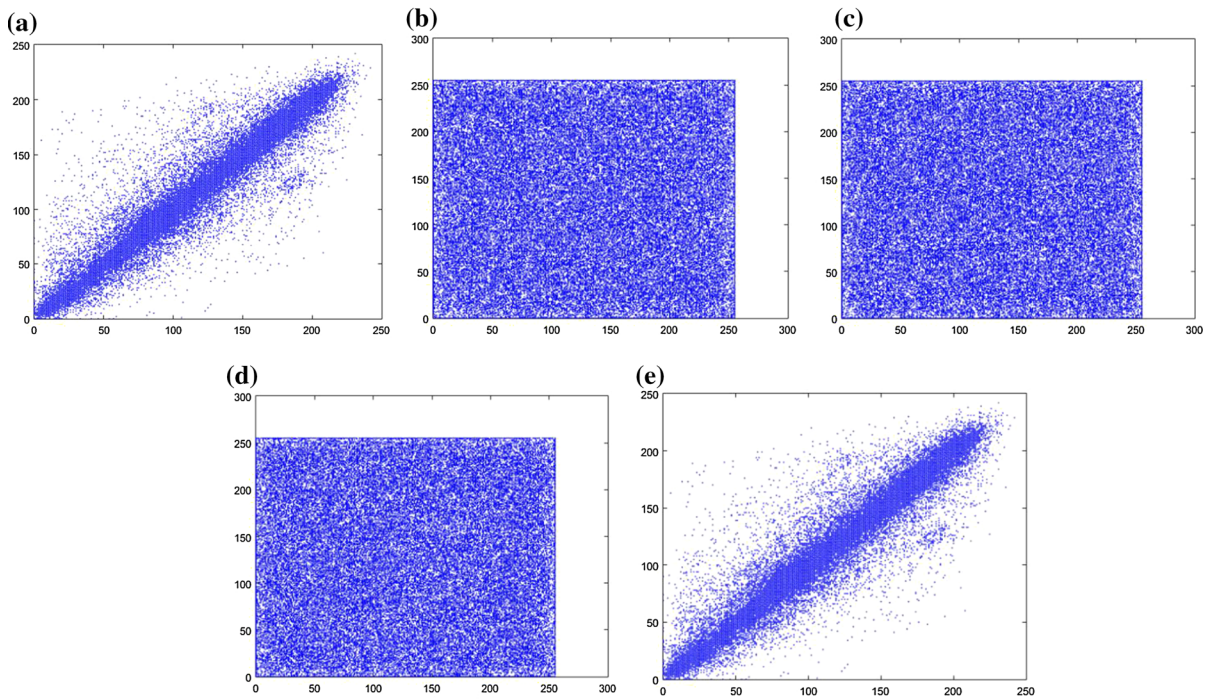

Fig. 13 The results of correlation analysis, **a** original image, **b** CL1 encrypted image, **c** CL2 encrypted image, **d** CL3 encrypted image, **e** decrypted image

Table 3 The security analysis results of encryption operations

	CL1	CL2	CL3
Information entropy	7.9558	7.9557	7.9538
Correlation	0.5197	0.5204	0.5176
NPCR	99.6353	99.5865	99.5789
UACI	29.5263	29.5724	29.7033

Table 3 shows that the NPCR values of the encryption processes performed in the study are very close to the optimum value.

$$\text{NPCR}(A, B) = \left(\sum_{i,j} D(i, j) / N \right) \times 100\%$$

$$D(i, j) = \begin{cases} 1 & \text{if} \quad A(i, j) \neq B(i, j) \\ 0 & \text{if} \quad A(i, j) = B(i, j) \end{cases} \quad (10)$$

The equation used to calculate the UACI value, which expresses the average intensity between two images, is given below. UACI optimal value is determined as $\text{UACI}_{opt} = 33.46\%$ [88]. When the UACI values of the encryption processes in Table 3 are examined, it is seen that these values are very close to the optimal values.

$$\text{UACI}(A, B)$$
$$= \frac{1}{N} \left(\sum_{i,j} (|A(i, j) - B(i, j)|) / 2^L - 1 \right) \times 100\%$$
$$(11)$$

Remark 1 It is very important to show that the generated chaotic systems can be applied to engineering problems as well as the production, analysis, and examination of dynamic behaviors of chaotic systems. In particular, chaotic systems are widely used in the design of random number generators and data security. However, there are many studies that only refer such applications [16–18,46,73,84,85,88]. In this study, RNG and image encryption applications were performed in this section to demonstrate the usefulness of different chaotic systems (CL1, CL2 and CL3) in engineering applications, and good enough results were obtained. Consequently, it was shown that the proposed chaotic systems can be employed in engineering applications.

6 Conclusion

In this paper, a new class of three-dimensional autonomous chaotic systems with equilibrium points like a three-leaved clover is presented. Dynamical specifications of these chaotic systems are demonstrated by the bifurcation diagrams, Lyapunov exponents, Kaplan-Yorke dimension, and Poincaré map. These chaotic flows belong to the recently proposed class of chaotic systems with hidden attractors. We hope that this paper can stimulate for the further study on chaotic systems with infinite number of equilibrium points like a three-leaved clover. A new RNG algorithm is designed using chaotic systems developed in the study, and NIST 800-22 randomness tests are applied to random bit sequences generated by the RNG algorithm. It has been found that all random bit sequences generated have high randomness and all NIST tests pass. Image encryption with random bit sequences is performed, and security analysis of the encryption process is performed. When security analysis results are evaluated, it is concluded that secure encryption is performed with bit sequences with high randomness. As a future work, the real circuit of the proposed system, due to its rich dynamical behavior, will be built for using it in a real "chaotic" application (encryption scheme). Moreover, it should be noted that the powerful robust control approaches such as robust tracking and model following [89–95], robust PID feedback [96,97], disturbance-observer-based robust control [98–101], robust linear matrix inequality (LMI) [102–106], robust H_{∞} control [107–109], sliding mode control [110–118], adaptive robust fuzzy control [119–124], terminal sliding mode control [125–131], and robust backstepping control [132–134] can be employed for the control or synchronization of this class of chaotic systems in the future researches.

References

1. Lorenz, E.N.: Deterministic nonperiodic flow. J. Atmos. Sci. **20**(2), 130–141 (1963)
2. Rössler, O.E.: An equation for continuous chaos. Phys. Lett. A **57**(5), 397–398 (1976)
3. Sprott, J.C.: Some simple chaotic flows. Phys. Rev. E **50**(2), R647 (1994)
4. Chen, G., Ueta, T.: Yet another chaotic attractor. Int. J. Bifurc Chaos **9**(07), 1465–1466 (1999)
5. Matsumoto, T.: A chaotic attractor from Chua's circuit. IEEE Trans. Circuits Syst. **31**(12), 1055–1058 (1984)
6. Linz, S.J., Sprott, J.: Elementary chaotic flow. Phys. Lett. A **259**(3), 240–245 (1999)
7. Lü, J., Chen, G.: A new chaotic attractor coined. Int. J. Bifurc. Chaos **12**(03), 659–661 (2002)
8. Pehlivan, İ., Uyaroğlu, Y.: A new 3D chaotic system with golden proportion equilibria: Analysis and electronic circuit realization. Comput. Electr. Eng. **38**(6), 1777–1784 (2012)
9. Chun-Ni, W., Jun, M., Run-Tong, C., Shi-Rong, L.: Synchronization and parameter identification of one class of realistic chaotic circuit. Chin. Phys. B **18**(9), 3766 (2009)
10. Gokyildirim, A., Uyaroglu, Y., Pehlivan, I.: A novel chaotic attractor and its weak signal detection application. Optik-Int. J. Light Electron Opt. **127**(19), 7889–7895 (2016)
11. Mobayen, S., Tchier, F.: Composite nonlinear feedback control technique for master/slave synchronization of nonlinear systems. Nonlinear Dyn. **87**(3), 1731–1747 (2017)
12. Asemani, M.H., Vatankhah, R.: Tracking control of chaotic spinning disks via nonlinear dynamic output feedback with input constraints. Complexity **21**(S1), 148–159 (2016)
13. Wang, C.-N., Ma, J., Jin, W.-Y.: Identification of parameters with different orders of magnitude in chaotic systems. Dyn. Syst. **27**(2), 253–270 (2012)
14. Jun, M., Wu-Yin, J., Yan-Long, L.: Chaotic signal-induced dynamics of degenerate optical parametric oscillator. Chaos, Solitons Fractals **36**(2), 494–499 (2008)
15. Fan, L., Chun-Ni, W., Jun, M.: Reliability of linear coupling synchronization of hyperchaotic systems with unknown parameters. Chin. Phys. B **22**(10), 100502 (2013)
16. Hussain, I., Shah, T., Gondal, M.A.: Application of S-box and chaotic map for image encryption. Math. Comput. Modell. **57**(9), 2576–2579 (2013)
17. Khan, M., Shah, T., Batool, S.I.: Construction of S-box based on chaotic Boolean functions and its application in image encryption. Neural Comput. Appl. **27**(3), 677–685 (2016)
18. Cao, Y.: A new hybrid chaotic map and its application on image encryption and hiding. Math. Probl. En. **2013**(Article ID 728375), 13 pages (2013)
19. Mobayen, S.: An LMI-based robust controller design using global nonlinear sliding surfaces and application to chaotic systems. Nonlinear Dyn. **79**(2), 1075–1084 (2015)
20. Mobayen, S.: Finite-time stabilization of a class of chaotic systems with matched and unmatched uncertainties: an LMI approach. Complexity **21**(5), 14–19 (2016)
21. Mobayen, S.: Design of LMI-based global sliding mode controller for uncertain nonlinear systems with application to Genesio's chaotic system. Complexity **21**(1), 94–98 (2015)
22. Mobayen, S., Tchier, F.: Synchronization of a class of uncertain chaotic systems with Lipschitz nonlinearities using state-feedback control design: a matrix inequality approach. Asian J. Control (2017). https://doi.org/10.1002/asjc.1512
23. Xi, X., Mobayen, S., Ren, H., Jafari, S.: Robust finite-time synchronization of a class of chaotic systems via adaptive global sliding mode control. J. Vib. Control, 1077546317713532 (2017)
24. Mobayen, S., Baleanu, D., Tchier, F.: Second-order fast terminal sliding mode control design based on LMI for a class of non-linear uncertain systems and its application to chaotic systems. J. Vib. Control **23**(18), 2912–2925 (2017)
25. Vaseghi, B., Pourmina, M.A., Mobayen, S.: Secure communication in wireless sensor networks based on chaos synchronization using adaptive sliding mode control. Nonlinear Dyn. **89**(3), 1689–1704 (2017)
26. Yongguo, Y., Yuhua, C., Qiuming, C.: Study on chaotic time series and its application on forecasting water inrush in mines. In: Geostatistical and Geospatial Approaches for the Characterization of Natural Resources in the Environment. pp. 95–99. Springer, Berlin (2016)
27. Liao, T.-L., Tsai, S.-H.: Adaptive synchronization of chaotic systems and its application to secure communications. Chaos, Solitons Fractals **11**(9), 1387–1396 (2000)
28. Cheng, C.-J.: Robust synchronization of uncertain unified chaotic systems subject to noise and its application to secure communication. Appl. Math. Comput. **219**(5), 2698–2712 (2012)
29. Liu, Y., Li, L., Feng, Y.: Finite-Time Synchronization for High-Dimensional Chaotic Systems and Its Application to Secure Communication. J. Comput. Nonlinear Dyn. **11**(5), 051028 (2016)
30. Muthukumar, P., Balasubramaniam, P., Ratnavelu, K.: Sliding mode control design for synchronization of fractional order chaotic systems and its application to a new cryptosystem. Int. J. Dyn. Control **5**(1), 115–123 (2017)
31. Liu, H., Kadir, A., Li, Y.: Audio encryption scheme by confusion and diffusion based on multi-scroll chaotic system and one-time keys. Opt.-Int. J. Light Electron Opt. **127**(19), 7431–7438 (2016)
32. Zhao, F., Liu, Y., Shao, Z., et al.: A chaotic local search based bacterial foraging algorithm and its application to a permutation flow-shop scheduling problem. Int. J. Comput. Integr. Manuf. **29**(9), 962–981 (2016)
33. Aihara, K.: Chaos engineering and its application to parallel distributed processing with chaotic neural networks. Proc. IEEE **90**(5), 919–930 (2002)
34. Esmaeili-Najafabadi, H., Ataei, M., Sabahi, M.F.: Designing Sequence With Minimum PSL Using Chebyshev Distance and its Application for Chaotic MIMO Radar Waveform Design. IEEE Trans. Signal Process. **65**(3), 690–704 (2017)
35. Wei, Z., Sprott, J., Chen, H.: Elementary quadratic chaotic flows with a single non-hyperbolic equilibrium. Phys. Lett. A **379**(37), 2184–2187 (2015)
36. Vaseghi, B., Pourmina, M.A., Mobayen, S.: Finite-time chaos synchronization and its application in wireless sen-

sor networks. Trans. Inst. Measur. Control (2017). https://doi.org/10.1177/0142331217731617

37. Dadras, S., Momeni, H.R., Qi, G.: Analysis of a new 3D smooth autonomous system with different wing chaotic attractors and transient chaos. Nonlinear Dyn. **62**(1), 391–405 (2010)

38. Dadras, S., Momeni, H.R., Majd, V.J.: Sliding mode control for uncertain new chaotic dynamical system. Chaos, Solitons Fractals **41**(4), 1857–1862 (2009)

39. Ma, J., Wu, X., Chu, R., Zhang, L.: Selection of multi-scroll attractors in Jerk circuits and their verification using Pspice. Nonlinear Dyn. **76**(4), 1951–1962 (2014)

40. Wang, C., Chu, R., Ma, J.: Controlling a chaotic resonator by means of dynamic track control. Complexity **21**(1), 370–378 (2015)

41. Mofid, O., Mobayen, S.: Adaptive synchronization of fractional-order quadratic chaotic flows with non-hyperbolic equilibrium. J. Vib. Control (2017). https://doi.org/10.1177/1077546317740021

42. Li, C.-L., Xiong, J.-B.: A simple chaotic system with non-hyperbolic equilibria. Opt.-Int. J. Light Electron Opt. **128**, 42–49 (2017)

43. Azar, A.T., Volos, C., Gerodimos, N.A., et al.: A novel chaotic system without equilibrium: dynamics, synchronization, and circuit realization. Complexity **2017**(Article ID 7871467), 11 pages (2017)

44. Pham, V.-T., Jafari, S., Volos, C.: A novel chaotic system with heart-shaped equilibrium and its circuital implementation. Opt.-Int. J. Light Electron Opt. **131**, 343–349 (2017)

45. Singh, J.P., Roy, B.: The simplest 4-D chaotic system with line of equilibria, chaotic 2-torus and 3-torus behaviour. Nonlinear Dyn. **89**(3), 1845–1862 (2017)

46. Chen, E., Min, L., Chen, G.: Discrete chaotic systems with one-line equilibria and their application to image encryption. Int. J. Bifurc. Chaos **27**(03), 1750046 (2017)

47. Jafari, S., Sprott, J.: Simple chaotic flows with a line equilibrium. Chaos, Solitons Fractals **57**, 79–84 (2013)

48. Li, C., Sprott, J., Thio, W.: Bistability in a hyperchaotic system with a line equilibrium. J. Exp. Theor. Phys. **118**(3), 494–500 (2014)

49. Ma, J., Chen, Z., Wang, Z., Zhang, Q.: A four-wing hyperchaotic attractor generated from a 4-D memristive system with a line equilibrium. Nonlinear Dyn. **81**(3), 1275–1288 (2015)

50. Pham, V.T., Jafari, S., Volos, C., et al.: A chaotic system with infinite equilibria located on a piecewise linear curve. Opt.-Int. J. Light Electron Opt. **127**(20), 9111–9117 (2016)

51. Chen, Y., Yang, Q.: A new Lorenz-type hyperchaotic system with a curve of equilibria. Math. Comput. Simul. **112**, 40–55 (2015)

52. Wang, X., Pham, V.-T., Volos, C.: Dynamics, circuit design, and synchronization of a new chaotic system with closed curve equilibrium. Complexity **2017** (2017)

53. Gotthans, T., Petržela, J.: New class of chaotic systems with circular equilibrium. Nonlinear Dyn. **81**(3), 1143–1149 (2015)

54. Gotthans, T., Sprott, J.C., Petrzela, J.: Simple chaotic flow with circle and square equilibrium. Int. J. Bifurc. Chaos **26**(08), 1650137 (2016)

55. Pham, V.T., Jafari, S., Volos, C., Kapitaniak, T.: A gallery of chaotic systems with an infinite number of equilibrium points. Chaos, Solitons Fractals **93**, 58–63 (2016)

56. Tlelo-Cuautle, E., Fraga, L.G., Pham, V.T., et al.: Dynamics, FPGA realization and application of a chaotic system with an infinite number of equilibrium points. Nonlinear Dyn. **89**(2), 1129–1139 (2017)

57. Pham, V.-T., Volos, C., Vaidyanathan, S., Wang, X.: A Chaotic system with an infinite number of equilibrium points: dynamics, horseshoe, and synchronization. Adv. Math. Phys. **2016**(Article ID 4024836), 8 pages (2016)

58. Kingni, S.T., Pham, V.-T., Jafari, S., Woafo, P.: A chaotic system with an infinite number of equilibrium points located on a line and on a hyperbola and its fractional-order form. Chaos, Solitons Fractals **99**, 209–218 (2017)

59. Pham, V.-T., Jafari, S., Wang, X., Ma, J.: A chaotic system with different shapes of equilibria. Int. J. Bifurc. Chaos **26**(04), 1650069 (2016)

60. Barati, K., Jafari, S., Sprott, J.C., Pham, V.-T.: Simple chaotic flows with a curve of equilibria. Int. J. Bifurc. Chaos **26**(12), 1630034 (2016)

61. Wolf, A., Swift, J.B., Swinney, H.L., Vastano, J.A.: Determining Lyapunov exponents from a time series. Phys. D **16**(3), 285–317 (1985)

62. Borah, M., Singh, P.P., Roy, B.K.: Improved chaotic dynamics of a fractional-order system, its chaos-suppressed synchronisation and circuit implementation. Circuits, Syst. Signal Process. **35**(6), 1871–1907 (2016)

63. Bouali, S., Buscarino, A., Fortuna, L., et al.: Emulating complex business cycles by using an electronic analogue. Nonlinear Anal.: Real World Appl. **13**(6), 2459–2465 (2012)

64. Kingni, S.T., Pham, V.T., Jafari, S., et al.: Three-dimensional chaotic autonomous system with a circular equilibrium: analysis, circuit implementation and its fractional-order form. Circuits, Syst. Signal Process. **35**(6), 1933–1948 (2016)

65. Wu, X., He, Y., Yu, W., Yin, B.: A new chaotic attractor and its synchronization implementation. Circuits, Syst. Signal Process. **34**(6), 1747–1768 (2015)

66. Zhou, W.J., Wang, Z.P., Wu, M.W., et al.: Dynamics analysis and circuit implementation of a new three-dimensional chaotic system. Opt.-Int. J. Light Electron Opt. **126**(7), 765–768 (2015)

67. Banerjee, S.: Chaos Synchronization and Cryptography for Secure Communications: Applications for Encryption: Applications for Encryption. IGI Global Publishers, Hershey (2010)

68. Cicek, S., Uyaroglu, Y., Pehlivan, I.: Simulation and circuit implementation of sprott case H chaotic system and its synchronization application for secure communication systems. J. Circuits Syst. Comput. **22**(04), 1350022 (2013)

69. ŞAHİN, S., GÜZELİŞ, C.: A dynamical state feedback chaotification method with application on liquid mixing. J. Circuits, Syst. Comput. **22**(07), 1350059 (2013)

70. Volos, C.K., Kyprianidis, I.M., Stouboulos, I.N.: A chaotic path planning generator for autonomous mobile robots. Robot. Auton. Syst. **60**(4), 651–656 (2012)

71. Volos, C.K., Kyprianidis, I.M., Stouboulos, I.N.: Image encryption process based on chaotic synchronization phenomena. Sig. Process. **93**(5), 1328–1340 (2013)

72. Wang, B., Xu, H., Yang, P., et al.: Target detection and ranging through lossy media using chaotic radar. Entropy **17**(4), 2082–2093 (2015)

73. Fatemi-Behbahani, E., Ansari-Asl, K., Farshidi, E.: A new approach to analysis and design of chaos-based random number generators using algorithmic converter. Circuits, Syst. Signal Process. **35**(11), 3830–3846 (2016)

74. Yalcin, M.E., Suykens, J.A., Vandewalle, J.: True random bit generation from a double-scroll attractor. IEEE Trans. Circuits Syst. I Regul. Pap. **51**(7), 1395–1404 (2004)

75. Elwakil, A., Ozoguz, S.: Chaos in pulse-excited resonator with self feedback. Electron. Lett. **39**(11), 831–833 (2003)

76. Piper, J.R., Sprott, J.C.: Simple autonomous chaotic circuits. IEEE Trans. Circuits Syst. II Express Briefs **57**(9), 730–734 (2010)

77. Trejo-Guerra, R., Tlelo-Cuautle, E., Jimenez-Fuentes, J.M., et al.: Integrated circuit generating 3-and 5-scroll attractors. Commun. Nonlinear Sci. Numer. Simul. **17**(11), 4328–4335 (2012)

78. Trejo-Guerra, R., Tlelo-Cuautle, E., Jiménez-Fuentes, M., et al.: Multiscroll floating gate-based integrated chaotic oscillator. Int. J. Circuit Theory Appl. **41**(8), 831–843 (2013)

79. Pano-Azucena, A.D., Rangel-Magdaleno, J.J., Tlelo-Cuautle, E., et al.: Arduino-based chaotic secure communication system using multi-directional multi-scroll chaotic oscillators. Nonlinear Dyn. **87**(4), 2203–2217 (2017)

80. Koyuncu, I., Ozcerit, A.T., Pehlivan, I.: Implementation of FPGA-based real time novel chaotic oscillator. Nonlinear Dyn. **77**(1–2), 49–59 (2014)

81. Tlelo-Cuautle, E., Rangel-Magdaleno, J.J., Pano-Azucena, A.D., et al.: FPGA realization of multi-scroll chaotic oscillators. Commun. Nonlinear Sci. Numer. Simul. **27**(1), 66–80 (2015)

82. Tlelo-Cuautle, E., Pano-Azucena, A.D., Rangel-Magdaleno, J.J., et al.: Generating a 50-scroll chaotic attractor at 66 MHz by using FPGAs. Nonlinear Dyn. **85**(4), 2143–2157 (2016)

83. Buscarino, A., Corradino, C., Fortuna, L., et al.: Non-ideal behavior of analog multipliers for chaos generation. IEEE Trans. Circuits Syst. II Express Briefs **63**(4), 396–400 (2016)

84. Rukhin, A., Soto, J., Nechvatal, J., et al.: A Statistical Test Suite for Random and Pseudorandom Number Generators for Cryptographic Applications. Booz-Allen and Hamilton Inc, Mclean (2001)

85. Pareek, N.K., Patidar, V., Sud, K.K.: Image encryption using chaotic logistic map. Image Vis. Comput. **24**(9), 926–934 (2006)

86. Shannon, C.E.: Communication theory of secrecy systems. Bell Labs Tech. J. **28**(4), 656–715 (1949)

87. Biham, E., Shamir, A.: Differential cryptanalysis of DES-like cryptosystems. J. Cryptol. **4**(1), 3–72 (1991)

88. Wang, Y., Wong, K.W., Liao, X., et al.: A chaos-based image encryption algorithm with variable control parameters. Chaos, Solitons Fractals **41**(4), 1773–1783 (2009)

89. Mobayen, S., Majd, V.J.: Robust tracking control method based on composite nonlinear feedback technique for linear systems with time-varying uncertain parameters and disturbances. Nonlinear Dyn. **70**(1), 171–180 (2012)

90. Mobayen, S.: Robust tracking controller for multivariable delayed systems with input saturation via composite nonlinear feedback. Nonlinear Dyn. **76**(1), 827–838 (2014)

91. Mobayen, S.: Finite-time robust-tracking and model-following controller for uncertain dynamical systems. J. Vib. Control **22**(4), 1117–1127 (2016)

92. Mobayen, S.: Design of a robust tracker and disturbance attenuator for uncertain systems with time delays. Complexity **21**(1), 340–348 (2015)

93. Golestani, M., Mobayen, S., Tchier, F.: Adaptive finite-time tracking control of uncertain non-linear n-order systems with unmatched uncertainties. IET Control Theory Appl. **10**(14), 1675–1683 (2016)

94. Mobayen, S., Tchier, F.: A novel robust adaptive second-order sliding mode tracking control technique for uncertain dynamical systems with matched and unmatched disturbances. Int. J. Control Autom. Syst. **15**(3), 1097–1106 (2017)

95. Mobayen, S., Tchier, F., Ragoub, L.: Design of an adaptive tracker for n-link rigid robotic manipulators based on super-twisting global nonlinear sliding mode control. Int. J. Syst. Sci. **48**(9), 1990–2002 (2017)

96. Aguilar-Lopez, R., Martinez-Guerra, R.: Partial synchronization of different chaotic oscillators using robust PID feedback. Chaos, Solitons Fractals **33**(2), 572–581 (2007)

97. Zhang, H., Shi, Y., Mehr, A.S.: Robust static output feedback control and remote PID design for networked motor systems. IEEE Trans. Industr. Electron. **58**(12), 5396–5405 (2011)

98. Chen, M., Wu, Q., Jiang, C.: Disturbance-observer-based robust synchronization control of uncertain chaotic systems. Nonlinear Dyn. **70**(4), 2421–2432 (2012)

99. Lin, J.-S., Liao, T.-L., Yan, J.-J., Yau, H.-T.: Synchronization of unidirectional coupled chaotic systems with unknown channel time-delay: adaptive robust observer-based approach. Chaos, Solitons Fractals **26**(3), 971–978 (2005)

100. Aguilar-López, R., Martínez-Guerra, R.: Synchronization of a class of chaotic signals via robust observer design. Chaos, Solitons Fractals **37**(2), 581–587 (2008)

101. Chen, M., Shao, S.-Y., Shi, P., Shi, Y.: Disturbance-observer-based robust synchronization control for a class of fractional-order chaotic systems. IEEE Trans. Circuits Syst. II Express Briefs **64**(4), 417–421 (2017)

102. Mobayen, S.: Design of LMI-based sliding mode controller with an exponential policy for a class of underactuated systems. Complexity **21**(5), 117–124 (2016)

103. Majd, V.J., Mobayen, S.: An ISM-based CNF tracking controller design for uncertain MIMO linear systems with multiple time-delays and external disturbances. Nonlinear Dyn. **80**(1–2), 591–613 (2015)

104. Mobayen, S.: An LMI-based robust tracker for uncertain linear systems with multiple time-varying delays using optimal composite nonlinear feedback technique. Nonlinear Dyn. **80**(1–2), 917–927 (2015)

105. Mobayen, S.: Optimal LMI-based state feedback stabilizer for uncertain nonlinear systems with time-varying uncertainties and disturbances. Complexity **21**(6), 356–362 (2016)

106. Mobayen, S., Tchier, F.: An LMI approach to adaptive robust tracker design for uncertain nonlinear systems with

time-delays and input nonlinearities. Nonlinear Dyn. **85**(3), 1965–1978 (2016)

107. Vafamand, N., Asemani, M.H., Khayatiyan, A.: A robust L 1 controller design for continuous-time TS systems with persistent bounded disturbance and actuator saturation. Eng. Appl. Artif. Intell. **56**, 212–221 (2016)

108. Asemani, M.H., Yazdanpanah, M.J., Majd, V.J., Golabi, A.: H∞ control of TS fuzzy singularly perturbed systems using multiple Lyapunov functions. Circuits, Syst. Signal Process. **32**(5), 2243–2266 (2013)

109. Asemani, M.H., Majd, V.J.: A robust H∞-tracking design for uncertain Takagi–Sugeno fuzzy systems with unknown premise variables using descriptor redundancy approach. Int. J. Syst. Sci. **46**(16), 2955–2972 (2015)

110. Mobayen, S.: Design of CNF-based nonlinear integral sliding surface for matched uncertain linear systems with multiple state-delays. Nonlinear Dyn. **77**(3), 1047–1054 (2014)

111. Mobayen, S.: An adaptive chattering-free PID sliding mode control based on dynamic sliding manifolds for a class of uncertain nonlinear systems. Nonlinear Dyn. **82**(1–2), 53–60 (2015)

112. Mobayen, S., Baleanu, D.: Linear matrix inequalities design approach for robust stabilization of uncertain nonlinear systems with perturbation based on optimally-tuned global sliding mode control. J. Vib. Control **23**(8), 1285–1295 (2017)

113. Mobayen, S.: A novel global sliding mode control based on exponential reaching law for a class of underactuated systems with external disturbances. J. Comput. Nonlinear Dyn. **11**(2), 021011 (2016)

114. Mobayen, S., Tchier, F.: A new LMI-based robust finite-time sliding mode control strategy for a class of uncertain nonlinear systems. Kybernetika **51**(6), 1035–1048 (2015)

115. Mobayen, S., Baleanu, D.: Stability analysis and controller design for the performance improvement of disturbed nonlinear systems using adaptive global sliding mode control approach. Nonlinear Dyn. **83**(3), 1557–1565 (2016)

116. Aghababa, M.P.: Robust stabilization and synchronization of a class of fractional-order chaotic systems via a novel fractional sliding mode controller. Commun. Nonlinear Sci. Numer. Simul. **17**(6), 2670–2681 (2012)

117. Mobayen, S., Tchier, F.: Design of an adaptive chattering avoidance global sliding mode tracker for uncertain nonlinear time-varying systems. Trans. Inst. Meas. Control, 0142331216644046 (2016)

118. Mobayen, S., Tchier, F.: Robust global second-order sliding mode control with adaptive parametertuning law for perturbed dynamical systems. Trans. Inst. Meas. Control (2017). https://doi.org/10.1177/0142331217708832

119. Liu, Y.-J., Zheng, Y.-Q.: Adaptive robust fuzzy control for a class of uncertain chaotic systems. Nonlinear Dyn. **57**(3), 431–439 (2009)

120. Hwang, E.-J., Hyun, C.-H., Kim, E., Park, M.: Fuzzy model based adaptive synchronization of uncertain chaotic systems: robust tracking control approach. Phys. Lett. A **373**(22), 1935–1939 (2009)

121. Poursamad, A., Davaie-Markazi, A.H.: Robust adaptive fuzzy control of unknown chaotic systems. Appl. Soft Comput. **9**(3), 970–976 (2009)

122. Wang, J., Qiao, G.-D., Deng, B.: Observer-based robust adaptive variable universe fuzzy control for chaotic system. Chaos, Solitons Fractals **23**(3), 1013–1032 (2005)

123. Chen, C.-S., Chen, H.-H.: Robust adaptive neural-fuzzy-network control for the synchronization of uncertain chaotic systems. Nonlinear Anal. Real World Appl. **10**(3), 1466–1479 (2009)

124. Mushage, B.O., Chedjou, J.C., Kyamakya, K.: An extended Neuro-Fuzzy-based robust adaptive sliding mode controller for linearizable systems and its application on a new chaotic system. Nonlinear Dyn. **83**(3), 1601–1619 (2016)

125. Mobayen, S.: Fast terminal sliding mode controller design for nonlinear second-order systems with time-varying uncertainties. Complexity **21**(2), 239–244 (2015)

126. Mobayen, S.: Fast terminal sliding mode tracking of nonholonomic systems with exponential decay rate. IET Control Theory Appl. **9**(8), 1294–1301 (2015)

127. Mobayen, S.: Finite-time tracking control of chained-form nonholonomic systems with external disturbances based on recursive terminal sliding mode method. Nonlinear Dyn. **80**(1–2), 669–683 (2015)

128. Mobayen, S., Javadi, S.: Disturbance observer and finite-time tracker design of disturbed third-order nonholonomic systems using terminal sliding mode. J. Vib. Control **23**(2), 181–189 (2017)

129. Mobayen, S.: An adaptive fast terminal sliding mode control combined with global sliding mode scheme for tracking control of uncertain nonlinear third-order systems. Nonlinear Dyn. **82**(1–2), 599–610 (2015)

130. Mobayen, S., Tchier, F.: Nonsingular fast terminal sliding-mode stabilizer for a class of uncertain nonlinear systems based on disturbance observer. Sci. Iran. **24**(3), 1410–1418 (2017)

131. Bayat, F., Mobayen, S., Javadi, S.: Finite-time tracking control of nth-order chained-form non-holonomic systems in the presence of disturbances. ISA Trans. **63**, 78–83 (2016)

132. Ji, D., Jeong, S., Park, J.H., Won, S.: Robust adaptive back-stepping synchronization for a class of uncertain chaotic systems using fuzzy disturbance observer. Nonlinear Dyn. **69**(3), 1125–1136 (2012)

133. Peng, C.-C., Chen, C.-L.: Robust chaotic control of Lorenz system by backstepping design. Chaos, Solitons Fractals **37**(2), 598–608 (2008)

134. Peng, Y.-F.: Robust intelligent backstepping tracking control for uncertain non-linear chaotic systems using H∞ control technique. Chaos, Solitons Fractals **41**(4), 2081–2096 (2009)